LAWRENCE
LIVERMORE
NATIONAL
LABORATORY

High Energy X-ray Source Generation by Short Pulse High Intensity Lasers

H-S. Park, J. A. Koch, O. L. Landen, T. W. Phillips, T. Goldsack, E. Clark, R. Eagleton, and R. Edwards

September 2, 2003

High Energy X-ray Source Generation by Short Pulse High Intensity Lasers

Hye-Sook Park*[a], Jefferey A. Koch[a], Otto L. Landen[a], Thomas W. Phillips[a], Tim Goldsack[b], Eugene Clark[b], Richard Eagleton[b], Ray Edwards[b]

[a]Lawrence Livermore Nationa Laboratory, 7000 East Avenue, Livermore CA, USA 94551-0808;
[b]AWE, Aldermaston, Reading, Berk Berkshire, RG7 4PR, UK

ABSTRACT

We are studying the feasibility of utilizing Kα x-ray sources in the range of 20 to 100 keV as a backlighters for imaging various stages of implosions and high areal density planar samples driven by the NIF laser facility. The hard x-ray Kα sources are created by relativistic electron plasma interactions in the target material after a radiation by short pulse high intensity lasers. In order to understand Kα source characteristics such as production efficiency and brightness as a function of laser parameters, we have performed experiments using the 10 J, 100 fs JanUSP laser. We utilized single-photon counting spectroscopy and x-ray imaging diagnostics to characterize the Kα source. We find that the Kα conversion efficiency from the laser energy at 22 keV is ~3 x 10^{-4}.

Keywords: Short pulse laser, Kα source, backlighter

INTRODUCTION

X-ray radiography using backlighter sources has been an important tool for diagnosing and imaging various stages of laser induced implosion. Until now, implosion experiments at Omega utilize <9 keV backlighter x-rays emitted by thermal plasmas generated from a target material. However, the larger and denser NIF targets will need an x-ray probe with energies of 20 to 100 keV to study their hydrodynamics, atomic structure, equations-of-state, and other properties (Ref).

An efficient high-energy x-ray radiography source can be created using an ultra-high-intensity laser, which produces high-energy non-thermal x-rays from interactions between relativistic electrons and cold target atoms. These electrons produce Kα fluorescence emission in any mid-to-high Z solid, and these 20-100 keV x-rays can be used as semi-mono energetic backlight sources for radiography. The construction of a multi-kJ, 1-10 ps Petawatt laser at the NIF is planned for generating adequate 20-100 keV x-rays for high-energy x-ray radiography applications.

However, we do not currently have a validated model that predicts x-ray source parameters for experimental conditions of interest. Previous experiments[1,2,3,4] to generate Kα mostly utilized low energy lasers that create a low intensity and fluence environment. A few experiments with Nova Petawatt laser[5,6] were able to reach 1x10^{19} W/cm^2 but Kα studies were limited to lower Z materials (Mo Kα at 17.5 keV). Because of the low laser x-ray intensities in these experiments, relativistic electron generation and propagation in solid targets is not well-understood; in particular, the physics affecting Kα production when transitioning from sub-ps low fluence conditions used in current experiments to the tens-of-ps high fluence conditions envisioned for NIF remains unexplored. X-ray conversion efficiencies, source sizes, time durations and spectral bandwidths at various x-ray energies, laser intensities, laser pulse durations, laser focal spot sizes, and target thickness remain to be quantified for source geometries of interest for radiography applications, such as foils, microdots and wires. Approaches to optimize various aspects of the source, such as the use of low-Z tamper layers, conical target geometries, and apertures also remain to be investigated. In addition, we need to develop imaging detectors and imaging optics that are appropriate to this high energy x-ray region. In order to investigate the characteristics of the Kα source

*park1@llnl.gov; phone 1 925 422-7062; fax 1 925 423-5517

generated from short pulse lasers, we began experiments using the JanUSP laser at LLNL and the Vulcan Petawatt laser at RAL.

JANUSP EXPERIMENTAL SET-UP
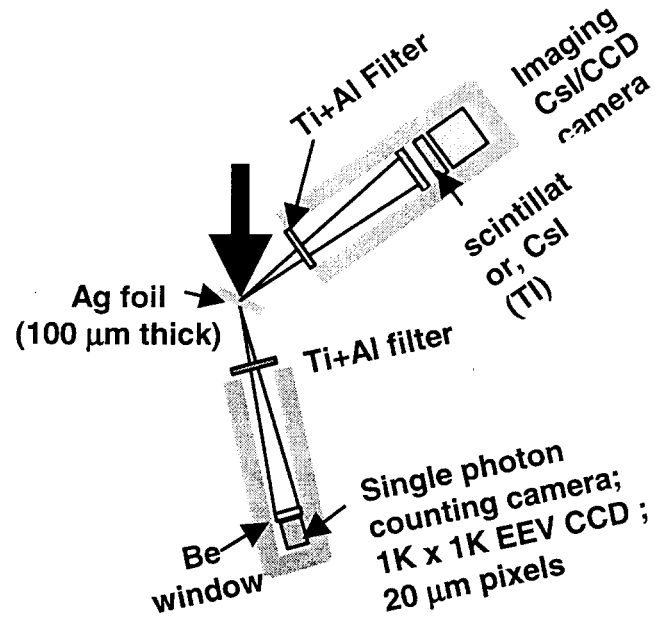
Figure 1. Schematic of experimental set-up for JanUSP laser to measure Silver Kα source properties. We employed 2 different detectors: direct x-ray exposure of a CCD array for single photon counting spectroscopy and an imaging camera with a CsI(Tl) scintillator.
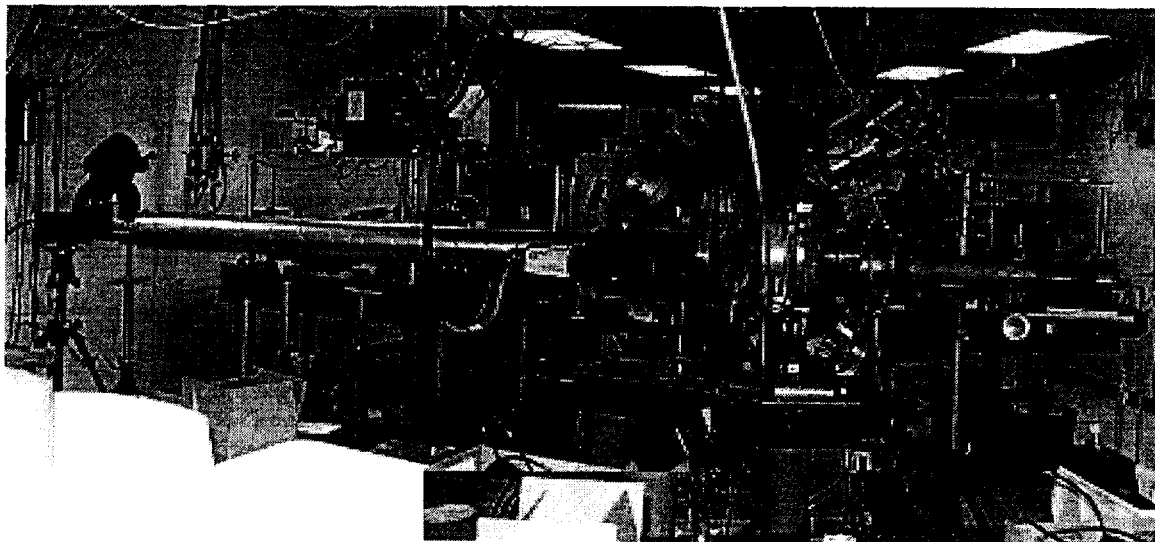
Figure 2. JanUSP experiment. The two ports of JanUSP chamber house the single photon counting camera and the x-ray imaging camera.

The JanUSP laser at LLNL can deliver up to 10 J of energy with 100 fs pulse duration and 4 μm diameter spot at a wavelength of 800 nm[7]. The short duration and small spot size produces intensities of up to 7×10^{20} Watt/cm^2. Though lower energy than the proposed NIF Petawatt laser, this laser can create similar intensities hence similar hot electron distribution. We performed initial experiments using JanUSP laser.

Figure 1 shows a schematic of our experimental set-up. The laser hits a 100 μm thick Ag target at ~45 degrees, and the reaction is monitored by two detectors. The first detector measures the x-ray spectrum through a single photon counting technique where a direct x-ray hit on a CCD produces electron-hole pairs that are proportional to the x-ray energy. The CCD is a 1300 x 1300 20 μm pixel CCD by EEV. This detector is placed 2.9 m away from the target center (TCC) with combined Ti and Al x-ray filters to attenuate the x-rays by a factor of 10 in order to avoid overlapping of the x-ray hits on the CCD. The second detector images the Kα source size and shape. The detector is a CCD camera coupled to a CsI (Tl doped) scintillator custom made by LLNL. Figure 2 shows the actual experimental setup.

EXPERIMENTAL DATA

| Entire CCD hit by X-ray photons | 100x100 pxl zoomed view of central region |
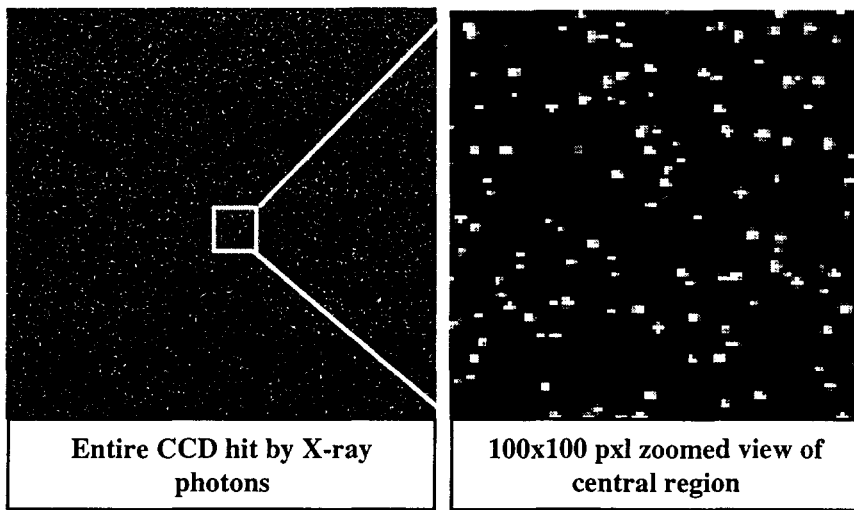
Figure 3. An image of x-ray hits from a laser interaction with a silver target. The intensity of each blob is proportional to the x-ray energy.

The Kα source production efficiency was measured using data from the single photon counting detector. Figure 3 shows an image taken during a laser shot. The first panel is the entire CCD and the second panel is a zoomed view of the central 100 x 100 pixel area. In the zoomed view, an x-ray hit is registered as a blob of connected pixels. Notice that the blobs are of different sizes and intensities represent the different x-ray photon energies.

For the analysis of this data we developed an algorithm that searches for the connected pixels, i.e. blobs, in these types of images and calculated the intensity of each blob. This algorithm first convolutes the pixilated image with a 2-dimensional Gaussian function that represents the best shape of the blobs. The Gaussian convolution works better than the x-ray summing up the pixel values over a defined boxed region because the x-ray hits are too close each other. The boxed sum intensity in a crowded field results in wrong intensities because the sums often include pixel values from neighboring x-ray hits. The resulting histogram of the intensities from a Gaussian convolution is shown in Figure 4.

In this figure the Kα and Kβ signals from the Ag target are clearly visible. The calibration of the digital camera units (SumADU) into absolute energy units (eV) was performed by two methods: the first was to expose the CCD to a 1.1mCi Cd109 isotope source that radiates Ag Kα (22 keV) and Kβ (24.9 keV) x-ray photons and 1.4 mCi Fe55 source that

radiates Mn Kα (5.9 keV). The same single photon counting and the Gaussian summation method were then applied to the resulting image to find the SumADU response to 5.9 keV, 22 keV and 24.9 keV x-rays. The results is shown in Figure 5. The second method was to calculate the expected signal from first principles. We know that the Si CCD band gap requires 3.65 eV to create an electron hole-pair and the camera's electronic gain is set to 1.1 electrons/ADU for our camera. From both methods we find that the conversion constant is 4.2 ADU/eV confirming our observation of the peaks at 5300 sumADU and 5900 sumADU to be the Ag Kα and Kβ peaks.
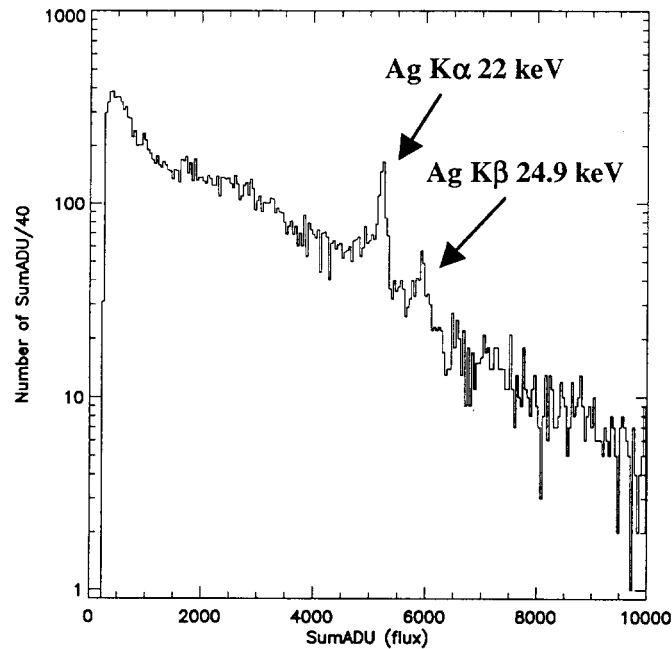
Figure 4. A histogram of blob intensity from the CCD directly exposed to the x-ray source. The Ag Kα and Kβ peaks are clearly detected above the backgrounds.
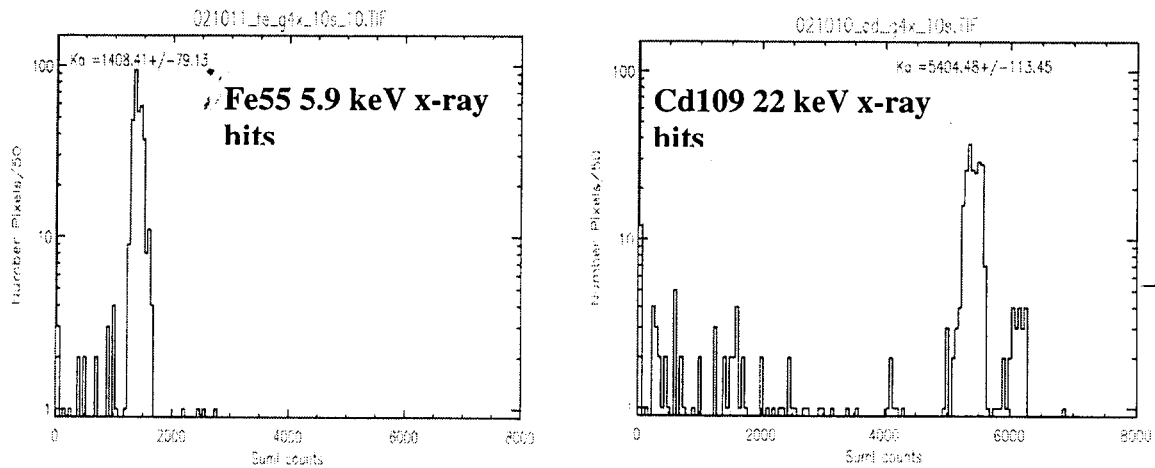
Figure 5. Single photon counting detector response to Fe55 and Cd109 isotope source. From this measurement, we calibrate the absolute scale of the SumADC to energy in eV.

22 KEV SILVER Kα SOURCE PRODUCTION EFFICIENCY

We calculate the conversion efficiency from laser energy to 22 keV Kα x-rays with our data. From the SumADU histograms such as in Figure 4, we fit the background near the 22 keV peak with a straight line. The background subtracted histogram is then fit to a Gaussian function whose fitting parameters are used to calculate the integrated area of the peaks. This integrated quantity represents the number of Kα x-rays observed in the data. This number is then corrected for the solid angle of the experimental set-up, the CCD 22 keV x-ray detection efficiency and the attenuation of the x-ray filters yielding the absolute total number of Kα generated in a laser shot. The conversion efficiency is the ratio of the total Kα energy to the total laser energy input. In the functional form:

$$\varepsilon_{conv} = \frac{K\alpha_{Total}}{E_{laser} / 22 \cdot keV}$$

$$K\alpha_{Total} = \frac{K\alpha_{Measured}}{DQE \cdot T_{filter} \cdot \Omega_{detector}} \cdot 4\pi$$

where ε_{conv} is the conversion efficiency, $K\alpha_{Total}$ is the total number Kα's into 4π, $K\alpha_{Measured}$ is the measured number of Kα's in our detector, DQE is detector detection efficiency at 22 keV, T_{filter} is transmission factor through the x-ray attenuation filter and $\Omega_{detector}$ is the detector solid angle.

The largest uncertainty in this measurement comes from the uncertainty in the DQE. The DQE is measured using the isotope source: we expose the detector for a specific time that provides the total number of x-ray photons. Then we count how many hits in our image. However, in this initial measurement, the number of x-ray photons is just a calculation from the estimated source strength instead of accurate measurement in the detector plane using a spectrometer. Also the source blockage was done manually preventing from more precise control of exposure time. With these uncertainties we estimate our error on the DQE to be accurate only within a factor of 2. Better measurement of the DQE is planned.
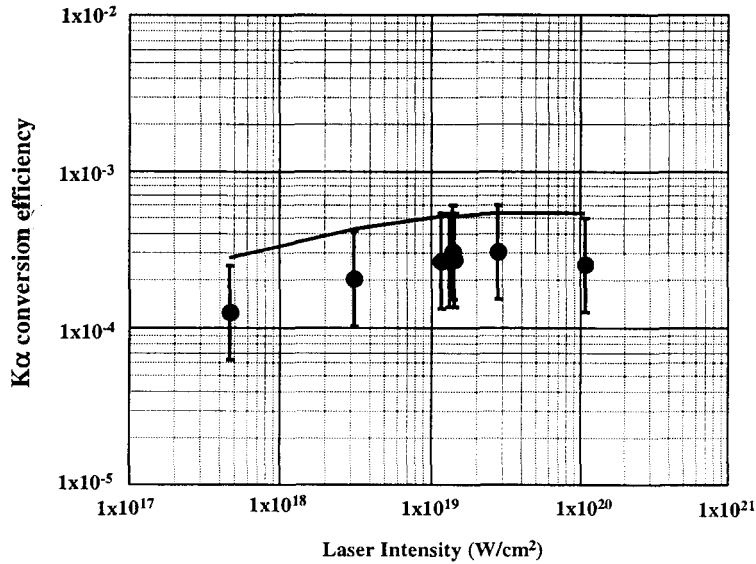

Figure 6 shows the final resulting conversion efficiency as function of laser intensity. Different laser intensities were obtained by varying the laser pulse duration or the spot sizes. The solid dots represent the data points and the line represents the Monte Carlo (MC) simulation.

The MC simulation of Kα x-ray production proceeds in two steps. First, the hot electron temperature is determined from the formula $T_{hot} = 130$ keV ($I(W/cm^2)/10^{17})^{1/2}$ [8] at laser intensities of interest. The ITS Monte Carlo code is run using electrons with a Boltzman energy distribution of temperature T_{hot}. In the calculation these electrons are emitted at the surface of the solid target into a cone of half-angle 26° into the target. From this simulation the number of Kα x-ray per electron per steradian as a function of angle is determined. Then the yield of Kα x-rays per steradian can be determined from the energy of the laser in Joules times the conversion fraction of that energy into electrons divided by the average energy of the electrons, T_{hot}. The conversion fraction as a function of intensity is obtained from LLNL PW data[6].

Our data matches the simulation within a factor of 2. The only other Ag Kα experimental measurements were performed by Yu et al[2] using a 0.53 μm, 400 fs high contrast laser at up to 5×10^{18} W/cm² where they measured a Kα conversion efficiency of only 1×10^{-5} and a low hot electron temperature of <35 keV. Our conversion efficiency is considerably higher than Yu's measurement.

CSI IMAGING CAMERA

In order to accommodate the x-ray imaging capability at this high energy, we developed a CCD camera that is coupled to a CsI (Tl doped) scintillator. The CsI(Tl) crystal was fabricated with columnar structure on a fiber optic face plate that provides higher imaging resolution than the regular slap crystal. This CsI scintillator plate is pressure mounted on a CCD camera with a fiber optic face plate. During the JanUSP experiment, we used this camera to image one laser shot with a 2 mm pinhole. The image is shown in Figure 7. The left panel is the image and the right panel is the vertical and horizontal lineouts. From this image, we found that the camera response was uniform within 3%. The spiky data points in the lineouts are mainly due to radiation hits that were excluded from the uniformity measurements. The Kα source size could not be directly imaged with a 2 mm pinhole with a magnification of 9. However, we analyzed the edge of this large penumbral image after taking into account of the thickness of the pinhole substrate and we measure the Kα source size may be 60±20 μm. More precise measurement of the Kα source with smaller pinholes (10-20 μm) is planned for next series experiment.
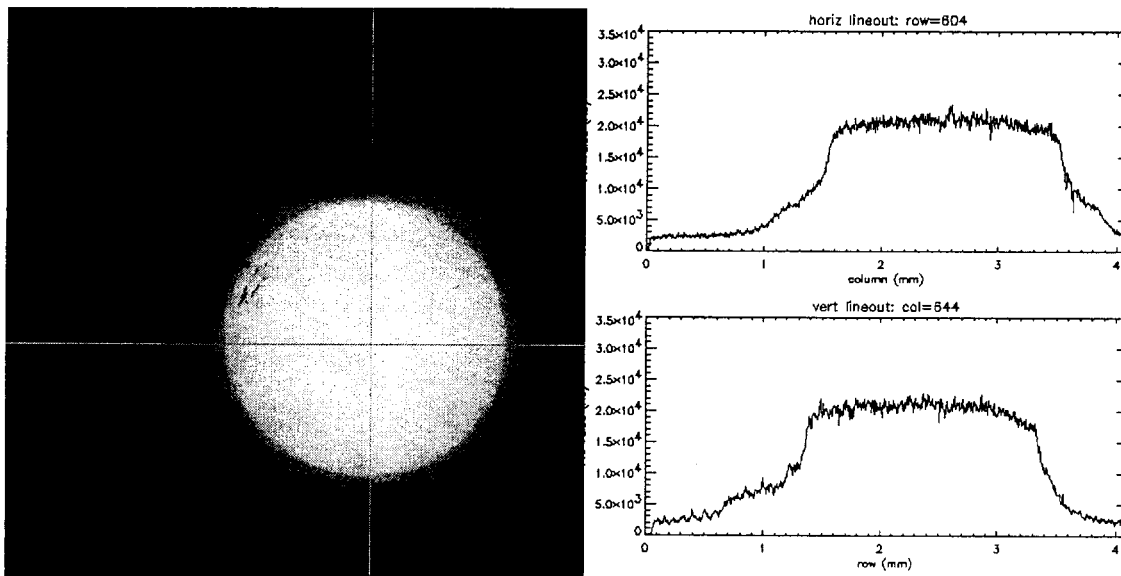
Figure 7. Penumbral image of Kα source from the JanUSP experiment. Preliminary analysis of this image show that the Ka source size is 60±20 μm. We used a CCD camera coupled with a CsI scintillator for this experiment.

CONCLUSION

We have measured the Kα conversion efficiency using the JanUSP laser at LLNL. At laser intensities of 1×10^{19} W/cm^2 the conversion efficiency is ~ 3×10^{-4}. This number agrees to within a factor of 2 with a theoretical prediction that utilizes an analytic hot electron temperature distribution function and the ITS Monte Carlo. We will repeat this experiment at the Vulcan Petawatt laser at Rutherford Appleton Laboratory which will deliver laser energies up to 250J. We are also planning to directly image Kα source with a CsI scintillator coupled CCD camera and a CdTe imaging detector.

ACKNOWLEDGMENTS

REFERENCES

1. Z. Jiang *et al.*, Phys. Plasmas **2**, 1702 (1995).
2. J. Yu *et al.*, Phys. Plasmas **6**, 1318 (1999).
3. E. Andersson *et al.*, J. Appl. Phys. **90**, 3048 (2001).
4. C. Tillman, *et al.*, Nuc. Instrum. Meth. Phys. Res. A **394**, 387 (1997).
5. K. Wharton, *et al.*, Phys. Rev. Lett. **81**, 822 (1998).
6. K. Yasuike, *et al.*, Rev. Sci. Instrum, **72**, 1236 (2001).
7. P. Springer, http://www.llnl.gov/str/Springer2.html
8. Ch. Reich *et al.*, Phys. Rev. Lett., **84**, 4846 (2000); Laser Part. Beams **19**, 147 (2001).